

# Comparison between observed and theoretical Red Giant Branch luminosity functions of galactic globular clusters<sup>\*</sup>

M. Zoccali and G. Piotto

Dipartimento di Astronomia – Università di Padova, Padova, Italy (zoccali,piotto@pd.astro.it)

Received 25 January 2000 / Accepted 26 April 2000

**Abstract.** *V*-band luminosity functions (LF) have been obtained for the upper main-sequence (MS), sub-giant branch (SGB) and red giant branch (RGB) of 18 galactic globular clusters (GGC) from HST data. A comparison with four sets of theoretical models has been performed. In contrast with what was found in several previous works, a good general agreement has been found between the observed and theoretical LF at any metallicity  $[M/H] < -0.7$ . Possible discrepancies at higher metallicity, in the upper part of the RGB, need to be confirmed with further observational data and by extending all the models to the most metal rich regime. The SGB shape has been used to set an upper limit to the cluster age, and consequently a lower limit on the cluster distance. A discussion on the still open problem of the mismatch between the observed and theoretical RGB bump location is also presented.

**Key words:** stars: distances – stars: evolution – stars: luminosity function, mass function – stars: Population II – Galaxy: globular clusters: general

## 1. Introduction

The luminosity function (LF) of a star cluster above the main sequence (MS) turnoff reflects primarily the rate of luminosity evolution. This happens because above the turnoff there is a rapid increase in the rate at which a star luminosity changes with time, and therefore these stars may be regarded as having started out with the same initial mass to within a few percent. The details of the interpretation of the evolved star LF in terms of the relevant stellar evolution theory, together with the many advantages of using the LFs to constrain the stellar models, have been excellently reviewed in a paper by Renzini & Fusi Pecci (1988).

In the present paper, we will focus our attention on the LF of the red giant branch (RGB), subgiant branch (SGB), and MS, excluding the horizontal branch (HB) and asymptotic giant

branch (AGB) stars, as well as the blue stragglers. Since the notation in the literature is not homogeneous, we point out that we will call SGB the region of the color magnitude diagram (CMD) that goes from the MS turnoff to just after the bend where the CMD starts to rise vertically. The RGB goes from this point up to the brightest stars. The LF of the RGB is a simple straight line on a magnitude- $\log(\text{counts})$  plane (cf. Fig. 1). The *slope* of this line allows a fundamental test of the evolutionary clock, i.e., of the rate at which stars ascend the RGB, and it is virtually independent of the cluster age or metallicity. The RGB LF also exhibits a characteristic bump, due to the hydrogen burning shell approaching the composition discontinuity left by the deepest penetration of the convective envelope. The level of agreement between the empirical and theoretical determination of the magnitude of the RGB bump, with respect to the HB level, for all the clusters of our database, has been analyzed in a dedicated paper (Zoccali et al. 1999), but it will be also discussed in the last section of this paper.

The SGB is certainly the most interesting part of the evolved-star LF, being the most sensitive to the stellar physical parameters. Due to the rapid increase in the number of stars towards the turnoff, and to the fact that the SGB is almost horizontal in the CMD, the SGB LF is mainly characterized by a steep drop (in the following called the SGB *break*) and by a peak just above the break (see Fig. 1 and Ratcliff 1987). The magnitudes at which these features occur depend mainly on age and metallicity (and of course also on the distance modulus in the observed LF). Both age and metallicity affect also the SGB shape, in a way that will be examined in the following. It is worth noting that the turnoff is *not* located at the break of the SGB, but it is  $\sim 0.5$  magnitudes fainter.

In the recent years, two unexpected results raised some questions on the ability of the models to predict the evolutionary rate out of the MS turnoff. In a LF obtained from the combination of the CCD-based LFs of the three metal-poor clusters M68 (NGC 4590), NGC 6397, and M92 (NGC 6341), Stetson (1991) found an excess of stars on the subgiant branch just above the main-sequence turnoff, the SGB *hump*, as it has been called by Faulkner & Swenson (1993). Later on, Bolte (1994) observed the metal-poor cluster M30 (NGC 7099) using a mosaic of small-field CCD images and found a similar excess of SGB stars. This excess has been investigated by several authors, both

---

Send offprint requests to: M. Zoccali (zoccali@pd.astro.it)

<sup>\*</sup> Based on observations with the NASA/ESA *Hubble Space Telescope*, obtained at the Space Telescope Science Institute, which is operated by AURA, Inc., under NASA contract NAS5-26555, and on observations retrieved from the ESO ST-ECF Archive.

theoretically and observationally. It has been suggested that it could be the observable result of an unusually extended isothermal core in turnoff stars, which could be produced by the actions of weakly interacting massive particles (WIMPs; Faulkner & Swenson 1993). More recently, different authors claimed that, at least for more metal-rich clusters, improved observations did not show the same effect (Sandquist et al. 1996; Degl'Innocenti et al. 1997).

The second unexpected observational evidence involving the LFs has been the disagreement between the theoretical and observed relative number of MS with respect to RGB stars. Several authors claimed that when a theoretical LF is normalized to the MS, there is an excess of observed giants relative to MS stars (Stetson 1991; Bergbusch & Vandenberg 1992; Bolte 1994; Degl'Innocenti et al. 1997). These results have been tentatively explained by the action of core rotation (Vandenberg et al. 1998). It must be noted that, at least in some cases, where the discrepancy is present at the faint end of the MS reached by the observational data, it could simply arise from a too steep exponent adopted for the mass function. In a more recent paper by Silvestri et al. (1998), new model LFs are presented, and a comparison of them with the observed LFs for the clusters M5 and NGC 6397 shows that no discrepancy is present. The authors argue that at least part of the disagreement claimed by previous authors could be due to a too rapid evolution of the stars on the RGB in the models previously used, which implies a predicted smaller number of RGB stars with respect to MS stars.

A discrepancy between observed and theoretical RGB LFs similar to that described above has been discussed more recently by Langer et al. (2000) for the two GGCs M5 and M30. They find an overabundance of red giants in the upper RGB of these two clusters, and they argue that the cause of this excess might be the action of deep mixing during the stars ascent along the RGB. This phenomenon (Sweigart 1997, 1998) should bring fresh fuel from the envelope into the hydrogen burning shell, causing a longer RGB lifetime and therefore an increase in the observed number of stars in that region. However, very little evidences support the claim that the stars in M5 and M30 may have experienced a stronger deep-mixing than other clusters that do not show similar RGB excess. In particular, a recent paper by Rood et al. (1999) demonstrates that the LF of M3, another cluster that, like M5, shows anomalous RGB abundances, interpreted as evidences of extra-mixing (Armosky et al. 1994) is in perfect agreement with the theoretical models by Straniero et al. (1997).

In summary, at the time we started this investigation, it was not clear whether the discrepancies between theory and observables described above were real and ubiquitous, if they were confined to some metallicity range, or if they were just an artefact due to observational uncertainties or to the properties of the different models used by different authors. Because of the potential importance of nonstandard physics in stars, and, more generally, in order to test the evolutionary rate predicted by the models, we decided to use the CMD database we have been creating in the last few years from our HST GO-6095, GO-

7470 and the ongoing GO-8118 snapshot survey and from the HST archive, in order to derive accurate LFs (with large number statistics) in a number of clusters.

There is an additional important reason why this investigation is worth: it has been suggested (e.g., Bergbusch & Vandenberg 1992) that the shape of the LF can be used to determine the absolute age of GGCs. However, we will show that this application is far from being straightforward, and the present investigation casts some doubts on the effectiveness of the LFs to get independent and accurate distances and ages.

For the sake of clearness, in Sect. 2 we will briefly summarize the effects of the main physical parameters of a star cluster — such as age, metallicity and the helium content — on the properties of the LFs. We will then critically discuss the most recent set of theoretical LFs, and justify the choice of the models that will be compared with the empirical data. In Sect. 3, we will present the observed LFs. A detailed comparison with the models will follow in Sect. 4. A general discussion of the implications of the present investigation can be found in Sect. 5.

## 2. The theoretical LFs

As anticipated above, the SGB is surely the most interesting part of the evolved-star LF, being the most sensitive to the stellar physical parameters. In particular, the metallicity, the age and, to a minor extent, the helium content affect both the position and the shape of the LF. It is important to discuss in more details this dependence, if we want to use the LF to estimate the cluster ages (see also Ratcliff 1987 and Bergbusch & Vandenberg 1992).

### 2.1. Position of the SGB break

In principle, the value of using the LFs to determine or constrain ages of GCs is due to the fact that the position of the SGB break is a strong function of age. Fig. 1a compares the LFs (from the models by Straniero et al. 1997), for  $t=10,12,14,16$  Gyr, for two extremes in metallicity  $[M/H]=-0.7, -1.7$ , and helium abundance  $Y=0.23$ . The LFs have been vertically normalized so that their RGBs coincide. The rate at which the break moves towards lower luminosities is essentially independent of chemical composition, but does decrease somewhat with increasing age. For clusters older than  $\sim 12$  Gyr, this rate is approximately 0.07 mag per Gyr, so that a determination of the location of this feature of the LF to within  $\sim 0.15$  mag means an age uncertainty of  $\sim 2$  Gyr. Unfortunately, one measures the *apparent* magnitudes of the stars, so that the distance modulus enters into the age determination as well, exactly as it does if one tries to measure GC ages via the turnoff absolute magnitude. In this sense, the only possible advantage of using the LF is that the magnitude of the break is easier to determine observationally, while the turnoff magnitude measured on a CMD is affected by an uncertainty of the order of a few tenths of a magnitude (Rosenberg et al. 1999). Apart from that, it must be noted that the position of the break *at a given age* is a function of chemical composition, too. Fig. 1b shows the  $t = 12$  Gyr LFs for  $Y=0.23$  as a function of metallicity. The values of the metallicity are indicated in the figure

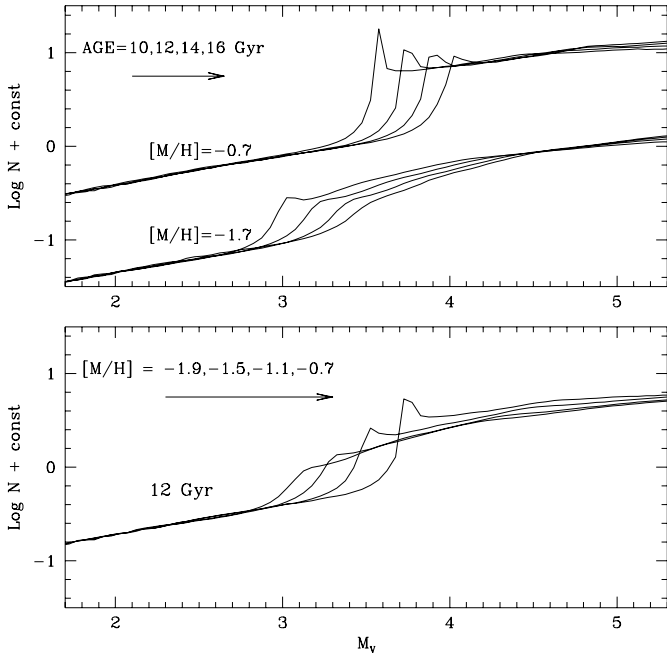


**Fig. 1.** Dependence of the magnitude of the SGB break of the LFs on the cluster age (top panel) and metallicity (bottom panel). The model LFs are from Straniero et al. (1997). A vertical shift has been allowed in order to make the RGB coincide.

label. The dependence on metallicity is stronger than on age, and increases with increasing metallicity. There is also a mild dependence of the break position on the helium content: for  $Y$  changing from 0.3 to 0.2 the break becomes  $\sim 0.1$  magnitudes brighter (Ratcliff 1987).

## 2.2. Shape of the SGB break

The slope of the SGB region of the LF is a strong function of the metallicity  $[M/H]$ , while the shape of the SGB (i.e., the sharpness of the peak) depends mainly on the age. Clearly, the RGB shape is independent of distance, making this part of the LF the most interesting for the absolute age determination (but see the discussion in Stetson 1991). Fig. 2 (top panel) shows how a change in  $[M/H]$  changes the slope and the shape of the SGB and turnoff region. Fig. 2 (bottom panel) shows that the age mainly affects the shape and the height of the peak, producing a very small change in the slope both before and after the peak, especially for metal-rich clusters. It must be noted, however, that beside the observational biases that we discuss in what follows, even from the theoretical point of view, the decrease in the sharpness of the SGB peak for decreasing metallicity makes the LFs of metal poor clusters less suitable for measuring the age from this feature. Note that in this figure the LFs has been registered allowing both a vertical and a horizontal shift, in order to match the position of their RGB and SGB break. The cause of the changes in the LFs seen in Fig. 2 can be better understood from Fig. 3, which show how the SGB region of the (theoretical) CMD is affected by a change in metallicity at a fixed age (top panel), and by a change in age at fixed metal-

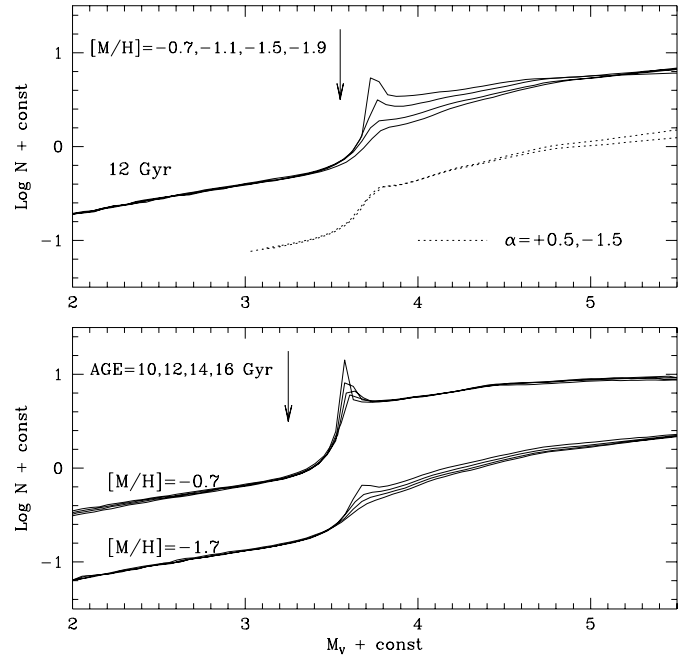


**Fig. 2.** Dependence of the shape of the SGB break of the LFs on the cluster metallicity (top panel) and age (bottom panel). Both vertical and horizontal shifts have been allowed in order to register the RGB and the magnitude of the break.

licity (bottom panel). A shift in color, in addition to the same magnitude shifts as in Fig. 2 has been applied in order to register the isochrone at the turnoff. The two dotted lines show the region corresponding to the SGB peak of the LF. It is clear from this figure that a change in age only affects the length of the horizontal part of the SGB, therefore the height of the SGB peak, while a change in metallicity has a stronger effect on the shape of the isochrone above the turnoff. The helium content affects mainly the height of the peak. However the relatively small uncertainties in the GGC helium content, combined with the small size of the effect, make the dependence on helium of no relevance in this paper. It is also worth noting that a change in the slope of the mass function would change the slope of the LF only below the turnoff, i.e.,  $\sim 1$  mag below the SGB break (Fig. 2 top panel, dotted lines). Therefore, different slopes of the SGB break and of the LF, from the break to about 1 magnitude fainter, are mainly due to different chemical compositions.

## 2.3. Choice of the reference models

All the models reproduce in a similar way the main features of the LFs discussed above. However, as one of the purposes of the present work is to test the predicted evolutionary rates, it is of some interest to compare the theoretical LFs published by different authors.

We considered the four most recent sets of theoretical LFs covering the whole range of metallicity spanned by our data. Fig. 4 shows the comparison of all of them, for three typical metallicities, an age of 10 Gyr. Table 1 summarizes the main input physics of the four sets of models. For a detailed descrip-

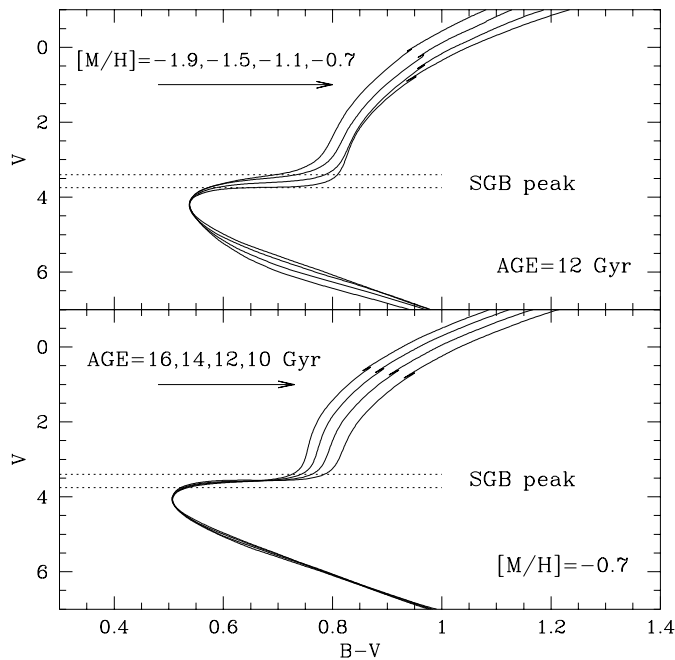


**Fig. 3.** Dependence of the shape of the SGB region, in the CMD, as a function of cluster metallicity (top panel) and age (bottom panel). Shifts in color, in addition to the same magnitude shift as in Fig. 2 have been applied in order to register the isochrones at the TO magnitude.

tion of each set of models we refer the reader to the relevant papers. As expected, the three models by Silvestri et al. (1998), Cassisi & Salaris (1997), and Straniero et al. (1997), which have been generated with very similar input physics, are almost indistinguishable from one another. The only difference worth noting is that the slope of the Silvestri et al.'s models slightly increases towards higher metallicity (see upper right panel). This fact will be further discussed when describing the observed LFs for the most metal-rich clusters. The models by Girardi et al. (1999) are slightly different from the others, both in predicting a larger number of MS with respect to the RGB stars, and a fainter RGB bump magnitude. While the cause of the former is not easy to identify, the latter is certainly due to the fact that Girardi et al. (1999) adopt overshooting at the lower boundary of the convective envelope, and therefore the envelope is bigger, the discontinuity in the hydrogen profile is closer to the center, and the shell encounters it earlier. As it will be discussed in the last section, these models seem to better reproduce the observed RGB bump position.

### 3. The data

All the LFs presented in this paper have been obtained from our photometric catalog, based on WFPC2 HST F439W and F555W data collected within our GO-6095, GO-7470, and GO-8118 programs, and from the HST archive. The CMDs for 32 of the 41 clusters observed so far can be found in Piotto et al. (1997), Sosin et al. (1997a), and Zoccali (1999). The details on the data reduction and calibration can be found in Piotto et al. (1999a). The same database has already been used for specific

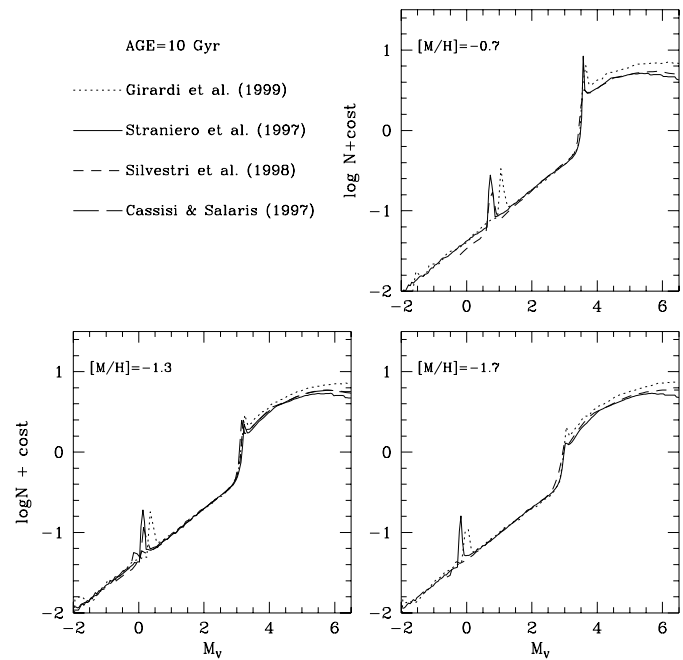


**Fig. 4.** Comparison among different sets of theoretical models. The LFs have been normalized to the region of the RGB between the RGB bump and the SGB break by allowing a vertical shift. All LFs refers to a mass function exponent of  $\alpha = -0.5$ .

investigations on the extended blue HBs (Piotto et al. 1999b), on the RGB bump (Zoccali et al. 1999), and on the helium content from the R parameter (Zoccali et al. 2000). All the data from the GO-6095 program published in Piotto et al. (1997), Sosin et al. (1997a), Sosin et al. (1997b), and Rich et al. (1997) have been reduced again using ALLFRAME (Stetson 1994). In the original preliminary reduction ALLSTAR (Stetson 1987) has been used. ALLFRAME allowed a slightly more accurate photometry towards the faintest part of the CMD and to extend it by  $\sim 1$  magnitude fainter.

Empirical LFs of the RGB+SGB+MS have been obtained for the 18 richest clusters of our database. Particular attention was devoted to estimating the completeness corrections, determined by means of artificial-star experiments. In order to optimize the use of cpu time, we need to add the maximum number of artificial stars without creating overcrowding, i.e., avoiding the overlap of two or more artificial-star profiles. To this purpose, as extensively described in Piotto & Zoccali (1999), the artificial stars were added in a spatial grid such that the separation of the centers in each star pair was two PSF radii plus one pixel. The relative position of each star was fixed within the grid, but in each successive experiment the magnitudes of the stars were chosen randomly and the grid was moved by a random amount. The input color for each artificial star was chosen according to the fiducial points representing the CMD, while the coordinate was transformed in order for the stars to occupy the same position in each frame. A total of  $\sim 4000$  stars were added (in five separate experiments) on each of the four WFPC2 chips. The coordinate of the input and output artificial-star lists were

**Table 1.** Main model input physics

Input physics	Straniero et al.	Cassisi & Salaris	Silvestri et al.	Girardi et al.
He diffusion	yes	no	no	no
EOS	Straniero 1988	Straniero 1988	OPAL	Straniero 1988
Nuclear rates	CF88 $^{12}C(\alpha, \gamma)^{16}O$ : C85	CF88 $^{12}C(\alpha, \gamma)^{16}O$ : C85	CF88	CF88 $^{12}C(\alpha, \gamma)^{16}O$ : 1.7×CF88
Convection	MLT Calib. from CSS95	MLT Calib. from SC96	FST DCM97	MLT Solar calib.
+ overshooting				
Colors	CGK97	CGK97	Kurucz 1993	Kurucz 1993

*References:* AF94: Alexander D.R. & Ferguson J.W. 1994, ApJ, 437, 879

Straniero O. 1988, A&AS, 76, 157 CF88: Caughlan G.R. & Fowler W.A. 1988, At. Data Nucl. Data Tables, 40, 283

C85: Caughlan G.R., Fowler W.A., Harris, M.J., & Zimmermann, B.A. 1985, At. Data Nucl. Data Tables, 32, 197

C95: Chieffi A., Straniero O. & Salaris M. 1995, ApJ, 445, L39

SC96: Salaris M. & Cassisi S. 1996, A&A, 305, 858

DCM97: D'Antona F., Caloi V. & Mazzitelli I. 1997, ApJ, 477, 519

CGK97: Castelli F., Gratton R.G. & Kurucz R.L. 1997, A&A, 318, 841

Kurucz R.L. 1993, CD-ROM 13 and CD-ROM 18

Buser R. & Kurucz R.L. 1978, A&A, 70, 555

then transformed in order to create a single field from a mosaic of the four WFPC2 chips. Finally, this field was divided into three radial annuli having approximately uniform density. The completeness fraction was assumed to be constant inside each annulus and estimated separately for each of them. Therefore, three LFs were obtained for each cluster. For the most concentrated clusters, with a strong stellar gradient, the three LFs have different magnitude limits, and blending effects may be present in the inner field. Only the LF points with completeness fraction above 50% are considered in the following.

The RGB LF was constructed as a histogram with a fixed bin size of 0.25 magnitudes. Since this region of the LF is featureless (except for the bump, whose properties do not change radially), and very similar in each radial annulus (due to the very small mass interval covered, the RGB stars are not affected by mass segregation), we summed the RGB LFs of the three annuli, in order to increase the statistics, and to better determine both the RGB slope and the bump location. The RGB LFs are shown as filled black dots, with errorbars, in Figs. 5–7. The errorbars include the Poisson errors and the uncertainty in the completeness correction. For the SGB and MS regions, we preferred to analyze separately the LFs of the different radial annuli, because they are affected to different extents by blending and incompleteness. Furthermore, in the faintest part of the MS, the observed LF can be affected by mass segregation, which brings the lighter stars towards the external regions, flattening the LF in the innermost annuli. Such effect is clearly visible in many of our clusters, but the explored mass range is too small (and too close to the limit magnitude) to allow a specific analysis on the cluster dynamical properties. Of course, errors in the completeness correction estimate could produce a similar effect on the LF.

In order to improve the magnitude resolution, the size of the bins of the SGB and MS LFs has been decreased with increasing number of stars. The y-coordinate of Figs. 5–7 represents the

**Table 2.** Cluster parameters

Cluster	[Fe/H]	[M/H]	c	$\mu_{0V}$	CMD
NGC 104	−0.68	−0.54	2.04	14.30	Sosin et al. (1997a)
NGC 362	−1.05	−0.84	1.94	14.67	Sosin et al. (1997a)
NGC1851	−1.14	−0.93	2.24	14.11	Sosin et al. (1997a)
NGC1904	−1.40	−1.19	1.72	16.15	Sosin et al. (1997a)
NGC2808	−1.24	−1.03	1.77	14.43	Sosin et al. (1997b)
NGC5694	−1.70	−1.49	1.84	16.17	
NGC5824	−1.69	−1.48	2.45	14.69	
NGC5927	−0.31	−0.17	1.60	15.48	Sosin et al. (1997a)
NGC5986	−1.52	−1.31	1.22	16.89	
NGC6093	−1.48	−1.27	1.95	14.76	
NGC6273	−1.53	−1.32	1.53	15.65	Piotto et al. (1999b)
NGC6356	−0.44	−0.30	1.54	16.06	
NGC6388	−0.53	−0.39	1.70	13.45	Rich et al. (1997)
NGC6624	−0.36	−0.22	pcc	14.45	Sosin et al. (1997a)
NGC6652	−0.86	−0.72	1.80	15.72	Sosin et al. (1997a)
NGC6934	−1.40	−1.19	1.53	16.99	Piotto et al. (1999a)
NGC6981	−1.40	−1.19	1.23	18.91	
NGC7078	−2.03	−1.82	pcc	14.06	Sosin et al. (1997a)

logarithm of the number of stars per unit magnitude interval. In all cases, the three plotted LFs correspond, from top to bottom, to the outer, intermediate and inner radial annulus.

#### 4. Comparison between observational and theoretical LFs

The LFs of each cluster are compared with a theoretical model appropriate for its metallicity. Table 2 shows the value of [Fe/H] in the Carretta & Gratton (1997) scale, as extended by Cohen et al. (1999). A mean enhancement of  $[\alpha/Fe]=0.2$  (for  $[Fe/H]> -1$ ) and  $[\alpha/Fe]=0.3$  (for  $[Fe/H]< -1$ ) was then applied to evaluate the global metallicity [M/H] (col. 3), which has been calculated using the relation given by Salaris et al. (1993). Table 2 also shows the concentration parameter (Harris 1996)

and the central surface brightness in the  $V$  band (Djorgovski 1993). The last column of Table 2 lists the papers where a CMD obtained from the same data has been presented.

For all the clusters, except the four most metal-rich ones (NGC 5927, NGC 6624, NGC 6356, and NGC 6388), we compared the empirical data only with the models by Straniero et al. (1997). As discussed in Sect. 2, a comparison with the models by Cassisi & Salaris (1997) and by Silvestri et al. (1998) would give identical results. As noted, the models by Girardi et al. (1999) are slightly different from the others, predicting a larger relative number of MS to RGB stars. Although for most of our data the errors do not allow us to exclude one or another theoretical prediction, some of our clusters clearly show a better agreement with the models that predict lower MS/RGB number ratio of stars. The Straniero et al. models have been chosen because they allowed the densest grid in metallicity. However, since these models do not cover the metal-rich tail of our data, for the four most metal-rich clusters we are forced to adopt the models by Silvestri et al. (1998), as extended into the most metal-rich regime by Ventura (priv. comm.).

In the comparison with the observed LFs, we adopted the following approach: 1) For each cluster we assumed the metallicity listed in Table 2; 2) Then we selected the age (using a grid with a 2 Gyr separation) choosing the theoretical LF best matching the peak of the SGB break; 3) Then we horizontally shifted the LF (i.e. found the apparent distance modulus) in order to match the SGB break; 4) The observed and theoretical LFs were finally vertically normalized to the total number of stars in the featureless RGB segment between the bump and the SGB.

When comparing the theoretical LFs with the observed ones, we must pay attention to the fact that there is a number of observational effects that can modify the observed LFs. Stetson (1991) has already discussed the possible effects of a small number statistics. However, the most important bias in the observed LF is due to the blending, which causes the identification of a single (brighter) star instead of two close fainter ones. In the CMD, this phenomenon produces a spurious binary sequence parallel to the MS, but brighter. In the LF this translates into a smearing of the main SGB features: the peak is lowered, the break is less steep, and there is an overabundance of stars at the base of the break. The latter feature corresponds to the brightest part of the “binary” sequence, between the base of the RGB and the blue stragglers (sometimes referred to as the “yellow straggler sequence”; Hesser et al. 1984). We will see that, even in the high resolution HST images, the effects of the blending appear quite clearly in many clusters. Typically, they are present in the inner, more crowded region, but gradually disappear in the outer part. As a consequence of blending we expect that *the age that we will obtain has to be considered only as an upper limit to the cluster age*. Indeed, beside other possible systematics, like uncertainty in the adopted metallicity scale, the only observational bias that could artificially increase the height of the SGB peak could be an error in the color term of the calibration equation that should distort the CMD making the SGB more horizontal. But such an effect would also make the slope of the observed

RGB significantly steeper than what was predicted by the models. We do not see any such effect in our comparisons. Finally, it is worth noting that the typical uncertainty in the cluster metallicity ( $\pm 0.15$  dex) translates into an uncertainty of  $\sim 1.5$  Gyr in the age determination (Fig. 2).

In any case, the main purpose of the present investigation is not the determination of the distance or age, though we will investigate how the LFs can constrain these parameters. Instead, we will test the agreement between the shape of the theoretical and observed LFs, in order to confirm or deny the claims of disagreement mentioned in the Introduction.

Figs. 5–7 show the comparison between the observed LFs with the best fitting theoretical ones. Note that the clusters have been ordered in terms of metallicity, starting from the most metal rich one. Table 3 summarizes the main results obtained for each cluster. Column 2 shows the radial intervals where the LFs were obtained ( $r < r_1$ ,  $r_1 < r < r_2$ ,  $r_2 < r < r_3$ ), col. 3 and 4 are the metallicity and the age of the theoretical model. The distance modulus required to match the SGB break and the difference between this distance and the value quoted in the Harris (1996) catalog are listed in col. 5. Finally col. 6 indicates whether the observed upper RGB LFs are reproduced by the models.

The models shown in Figs. 5–7 were all generated assuming a mass function with slope  $\alpha = -0.5$  (where Salpeter is  $\alpha = -2.35$ ). Such a flat mass function has been chosen because we are looking at the cluster cores, where mass segregation causes a flattening of the mass function. The only cluster for which a steeper mass function ( $\alpha = -2.5$ ) was required is NGC 5694. In almost all the GGCs for which deep enough data are available, the effect of mass segregations are visible in the fainter bins of the MS, the outer LF being steeper than the inner one (see e.g. NGC 7078).

## 5. Discussion

### 5.1. The SGB hump

It is clear from Figs. 5–7 that in general there is very good agreement between the observed and theoretical LFs. The number of stars in the SGB, and in general the shape of this region, is very well reproduced by the models. The only exceptions are the most internal regions of the most concentrated clusters (e.g., NGC 1851, NGC 2808, inner LFs) where the excess of stars just above the SGB break is entirely due to stellar blends, that brings MS stars towards brighter magnitudes. This phenomenon is illustrated in Fig. 8 from one of our artificial star experiments in the most crowded cluster NGC 6388. In this figure, the difference between the output and the input magnitude of the artificial stars is plotted against the output magnitude. The stellar blends, relatively more abundant in the intermediate annulus than in the external one, are those stars with negative values of  $V_{OUT} - V_{IN}$ , i.e., measured with a magnitude brighter than the original one. The vertical arrow marks the magnitude of the SGB break. At this magnitude level, in the intermediate annulus, about half of the stars are found in blends, while in the outer annulus this fraction is considerably reduced. Fig. 5 confirms that the LF for NGC 6388 is of poor quality, especially in

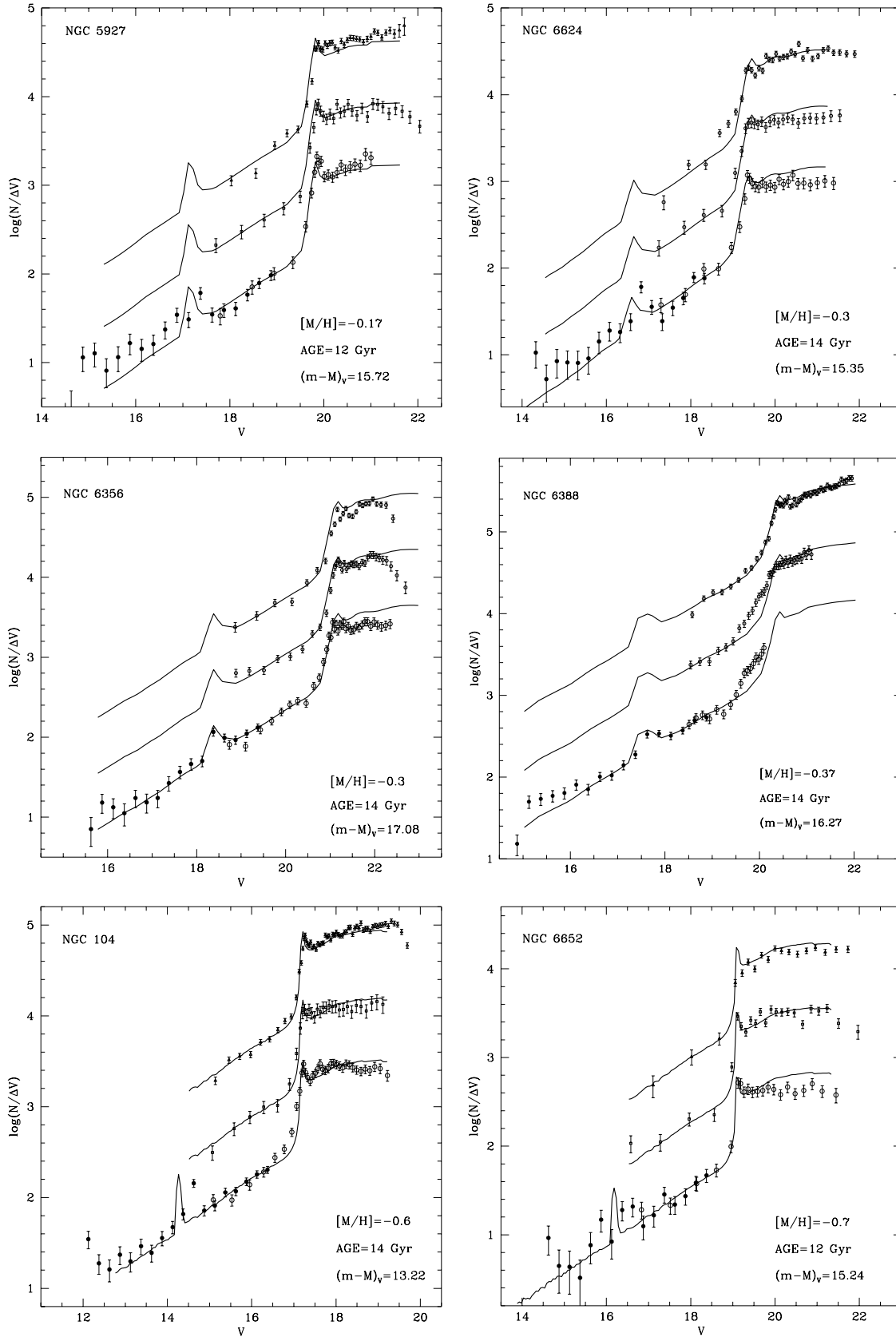


**Fig. 5.** The LFs in the three radial annuli (top to bottom: outer, intermediate and inner) for six GGCs of our database. The radial limits of the annuli are listed in Table 3. Overplotted solid lines show the theoretical model for the age and metallicity listed in the figure labels. The distance modulus required to match the observed and theoretical SGB break position is also quoted in the figure label.

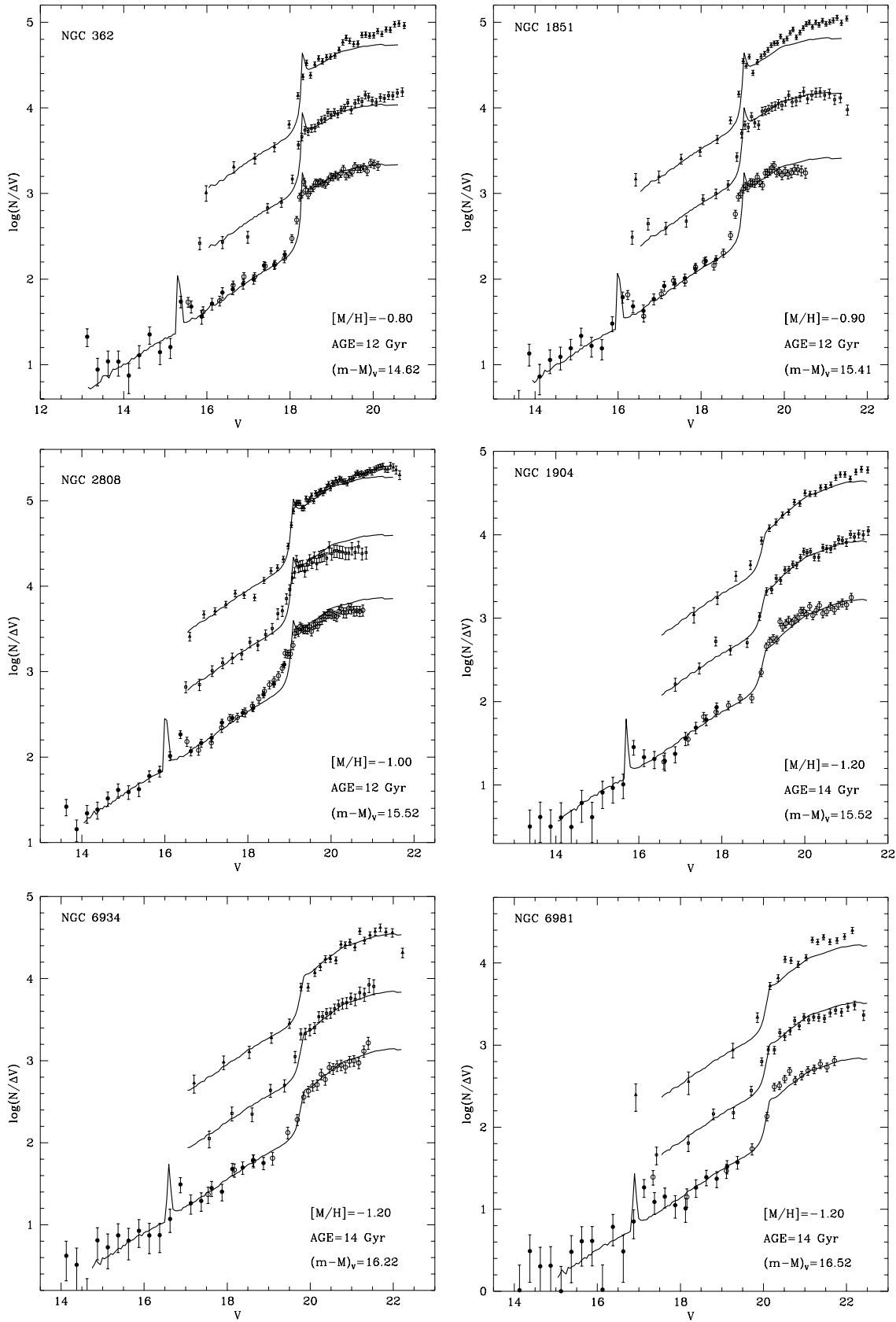


Fig. 6. Same as Fig. 5, for other six GICs of the database.

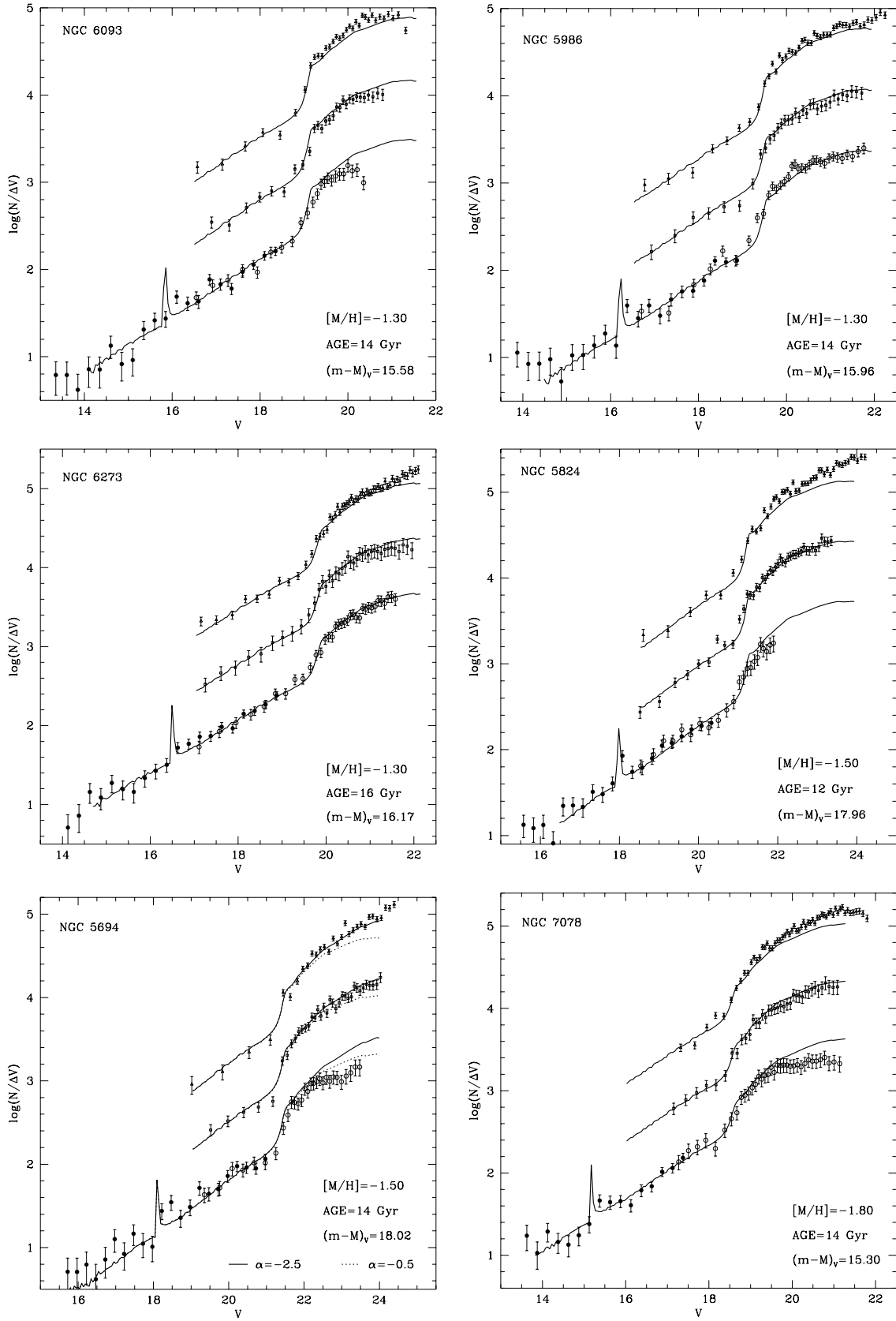
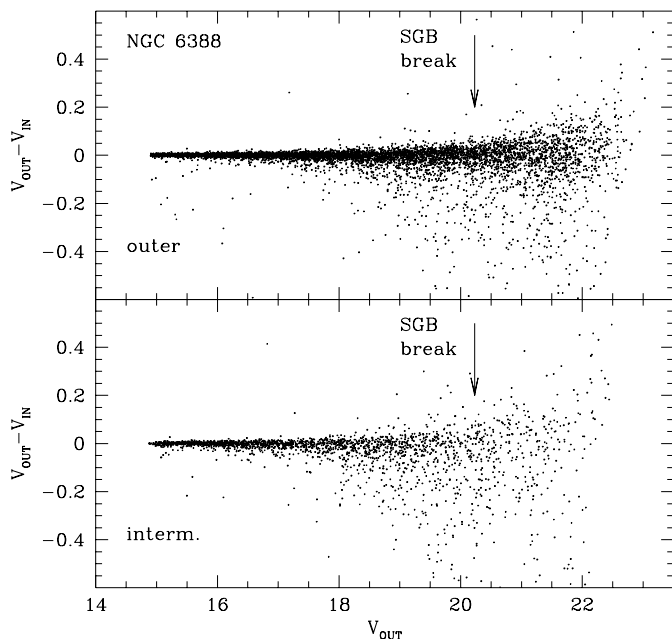


Fig. 7. Same as Fig. 5, for other six GICs of the database.

**Table 3.** Summary of results

Cluster	$r_1, r_2, r_3$	[M/H] (arcsec)	AGE (Gyr)	$(m - M)_V$ (mag)	$\Delta(m - M)_V$ (mag)	upper RGB
NGC5927	25,50,120	-0.17	12	15.72	-0.09	no
NGC6624	15,40,120	-0.30	14	15.35	-0.02	no
NGC6356	25,70,120	-0.30	14	17.08	0.31	yes
NGC6388	20,50,120	-0.37	14	16.27	-0.27	no
NGC 104	20,40,120	-0.60	14	13.22	-0.15	yes?
NGC6652	15,50,120	-0.70	12	15.24	0.05	yes
NGC 362	30,60,120	-0.80	12	14.62	-0.18	yes
NGC1851	25,50,120	-0.90	12	15.41	-0.06	yes?
NGC2808	25,50,120	-1.00	12	15.52	-0.04	yes
NGC1904	25,60,120	-1.20	14	15.52	-0.07	yes
NGC6934	18,50,120	-1.20	14	16.22	-0.26	yes?
NGC6981	25,60,120	-1.20	14	16.52	0.21	yes
NGC6093	15,45,120	-1.30	14	15.58	0.02	yes
NGC5986	25,50,120	-1.30	14	15.96	0.02	yes
NGC6273	25,50,120	-1.30	16	16.17	0.32	yes
NGC5824	13,45,120	-1.50	12	17.96	0.03	yes
NGC5694	13,45,120	-1.50	14	18.02	0.04	yes?
NGC7078	15,40,120	-1.80	14	15.30	-0.07	yes



**Fig. 8.** Difference between the input and output magnitude of the artificial star experiments on the intermediate (lower panel) and outer (upper panel) annuli of NGC 6388. The vertical arrow marks the location of the SGB break in the LF. Note that the dispersion of the data is not symmetric, and the effect is more pronounced in the intermediate annulus.

the innermost regions. The cause of this is partially due to the presence of both total and differential reddening that broadens the CMD sequences (see Rich et al. 1997), but the excess of stars above the SGB break is clearly due to crowding, since it gradually disappears towards the outer part.

We conclude that our data do not support the claims of the presence of a SGB hump. We believe that the most plausible explanation for this effect is the presence of stellar blends, strongly affecting most ground-based studies.

### 5.2. The ratio of MS/RGB stars

The observed number of MS/RGB stars is in agreement with theoretical predictions, within the uncertainties. As concluded by Degl'Innocenti et al. (1997), minor deviations in some cases (e.g. NGC 6981, outer LF) are more likely the consequence of mass segregation, or of residual errors in the completeness corrections or simply to small number statistics along the RGB were the LFs were normalized, than real features to ascribe to a mismatch with theory. Indeed, such discrepancies disappear in the most internal, richest LFs. Of course we cannot exclude the possibility of a real radial gradient in the number ratio of MS/RGB stars, but this hypothesis does not seem very plausible and would require further tests with wider radial coverage.

### 5.3. The upper RGB

The problem of the upper RGB is more complicated. At variance with what was found by Langer et al. (2000), we do not find any systematic excess of RGB stars for  $[M/H] > -0.7$ . Some excess of RGB stars similar to that found by Langer et al. (2000) is visible for the clusters NGC 6652, NGC 1851, NGC 6934, and NGC 5694, but in *all* these cases the theoretical models agree with the data within the errors, so these discrepancies are not significant. In the more metal rich regime ( $[M/H] < 0.7$ ), and in particular for NGC 5927, NGC 6624 and NGC 6388, we find systematic deviations of different nature. While Langer et al. (2000) find a displacement of the observed

LF with respect to the theoretical one, for these three clusters we find that the observed upper RGB slopes are flatter than the theoretical ones. It must be noted that in this interval we used a different set of models (Silvestri et al. 1998), which become steeper and steeper in the upper RGB with increasing metallicity (cf. Fig. 4). It would be interesting to verify whether also the other models show the same behaviour in the most metal-rich regime. In any case, this slope change is much smaller than the observed discrepancy between data and theory (Fig. 5). Possible alternative explanations are: 1) contamination by AGB stars, 2) the presence of differential reddening, and 3) problems with the bolometric corrections adopted in the models. We exclude the first two possibilities. Indeed, the expected number of AGB stars (most of which have been excluded from the LF) cannot explain a difference by a factor of two, as observed in the upper bins of the most metal rich clusters of Fig. 5. We have also performed numerical experiments to test the second possibility, and found that the presence of differential reddening causes a smoothing of the LF main features but not a change in its slope. Instead, the fact that the deviation between observations and theory is confined to a gradually smaller and brighter magnitude interval for decreasing metallicity, suggests that this mismatch could be due to problems in the bolometric correction. Indeed, as shown in Ortolani et al. (1990, 1992), the upper RGB for the most metal rich clusters in the  $V$  vs.  $(B - V)$  plane turns down due to blanketing effects. As already discussed by Ortolani et al. (1990), and verified also for the models adopted here, even the most recent bolometric corrections are not able to correctly reproduce this feature in the CMD. For the same reason, we expect that also the theoretical LFs for the most metal rich clusters cannot match the observed data in brightest bins. In view of the potential implications of this discrepancy in terms of the evolutionary lifetime in the upper RGB of metal-rich clusters, this effect deserves further investigations.

#### 5.4. Distances and Ages

The approach we followed in the comparison between the observed and theoretical LFs has been to *measure* the age from the shape of the SGB peak, and then to derive the distance modulus required to match the SGB break at that fixed age. As we discussed in Sect. 2 this is not the best method to measure cluster ages and distances, since it is strongly affected by the quality of the photometric data. Still, it might be of some interest to compare the distances obtained from our LFs with the ones in the literature. In the *lower panel* of Fig. 9, we compare our distance moduli with the values in the most updated Harris's catalog (June 22<sup>nd</sup>, 1999 revision;

<http://physun.physics.mcmaster.ca/GC/mwgc.dat>). It is reassuring that there is a general agreement between the two sets of distances. The average difference is:  $(m - M)_V^{LFs} - (m - M)_V^{HARRIS} = -0.01 \pm 0.15$ , and the residuals show no trend with the metallicity. The logic consequence of this agreement is that also the ages should be on average correct. The *upper panel* of Fig. 9 shows the ages found for each cluster with the method described above. The average age is 13 Gyr, while the

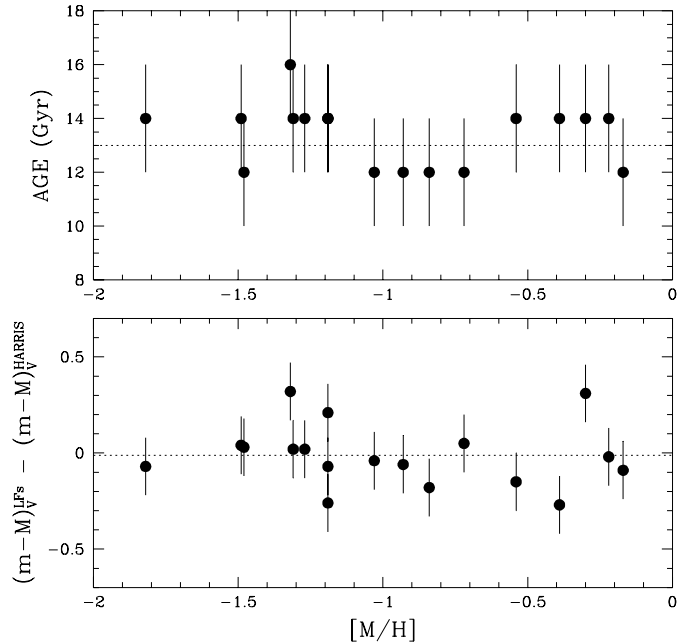


**Fig. 9.** *Upper panel:* the measured cluster ages as a function of metallicity. *Lower Panel:* the difference between the distance moduli of the studied clusters given in Harris's catalogue, and the distance moduli determined from the comparison between the observed and the theoretical LFs.

dispersion is of the same order of the error bars, and there is no age trend with the metallicity. Keeping in mind the large uncertainty related to our age determination, it is of some interest to note that we have the same result on GGC relative ages as in Rosenberg et al. (1999).

#### 5.5. The RGB bump

Another feature of the observed LF that must be compared with theoretical models is the RGB bump. There have been claims that the observed position of the RGB bump is not well reproduced by theoretical models. The first time that this feature was clearly identified in a GGC (King et al. 1985), its position was found to be 0.85 magnitudes fainter than predicted by the models of Sweigart & Gross (1978). Later on, in a dedicated paper, Fusi Pecci et al. (1990) found a smaller average discrepancy ( $\sim 0.42$  magnitudes) from the comparison of a large sample of data (11 GGCs) with the models by Rood & Crocker (1989). More recently, Cassisi & Salaris (1996) and Zoccali et al. (1999) showed that, adopting the new metallicity scale by Carretta & Gratton (1997) and taking into account a modest alpha-element enhancement, the observed magnitude difference between the bump and the HB ( $\Delta V_{HB}^{Bump}$ ) is in good agreement with canonical theoretical models that include the most updated input physics.

Although it is true that the  $\Delta V_{HB}^{Bump}$  is well reproduced by the models, Figs. 5–7 clearly shows that the absolute magnitude of the theoretical RGB bump is still systematically brighter than the observed one by  $\sim 0.25$  mags. Of course, the level of

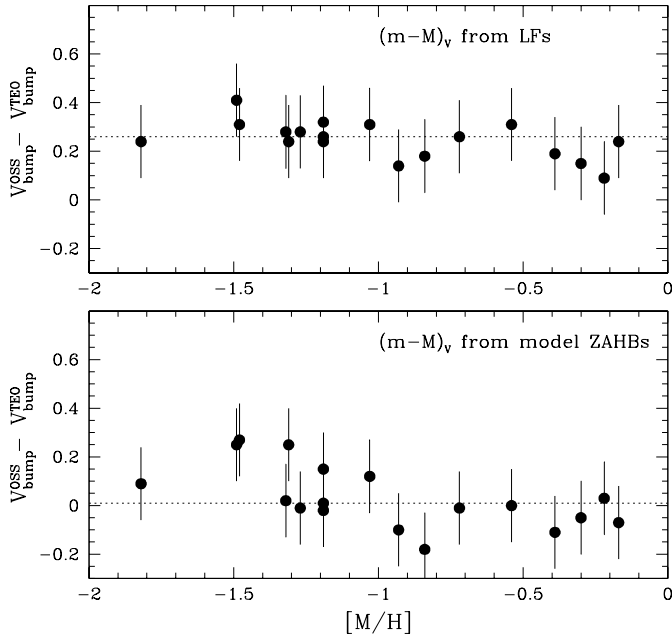


**Fig. 10.** Difference between the observed and theoretical location of the RGB bump, as a function of metallicity, for two different assumption on the distance. Top panel: the adopted distance moduli have been determined via the comparison between theoretical and observed LFs. Bottom panel: the distance moduli come from the comparison between observed and theoretical ZAHBs.

agreement between the theoretical and empirical bump location strongly depends on the adopted distance modulus. We already showed that our derived distance moduli are on average in good agreement with the values obtained with the distance scale adopted in Harris's catalog (Fig. 9).

Only the models by Girardi et al. (1999) are able to correctly locate the bump. However, it is worth noting that this result has been obtained by including in the models an additional free parameter, i.e., some overshooting at the base of the convective envelope (Bressan et al. 1981).

Fig. 10 (*upper panel*) shows that the theoretical magnitude of the bump as predicted by the LFs of Straniero et al. (1997) and Silvestri et al. (1998) is systematically brighter by 0.26 mags. On the other hand, the fact that the observed  $\Delta V_{HB}^{Bump}$  is in good agreement with the theoretical predictions suggests that adopting the distance modulus obtained from the theoretical absolute magnitude of the zero age horizontal branch (ZAHB), we are able to remove this discrepancy.

Indeed, from a comparison between the theoretical ZAHB location (Salaris & Cassisi 1998):

$$M_V^{ZAHB} = 0.974 + 0.379 \times [M/H] + 0.062 \times [M/H]^2$$

and the empirical ZAHB magnitudes of Zoccali et al. (1999), we would obtain systematically longer distances (by  $\sim 0.26$  mag) and therefore a very good match of the position of the RGB bump (Fig. 10, *lower panel*). It must be noted that the distances are also

systematically longer than the values in the Harris catalog<sup>1</sup>, but more consistent with the HIPPARCOS distance scale (Salaris & Weiss 1998).

Of course, adopting the longer distance scale implies a  $\sim 2$ –4 Gyr younger age for all the clusters. Then one is left with the impression that, if the SGB shape and the ZAHB give different results for the age and the distance, there must be some internal inconsistency in the theoretical models. However, such a conclusion is premature, given that the ages measured via the SGB shape must be considered only an upper limit, therefore the LF approach do not allow us to exclude younger ages and longer distances, as required to fit the ZAHB models (and the RGB bump).

## 6. Conclusions

We obtained the LFs for the RGB+SGB+MS of a sample of 18 GGCs, observed with HST, with the main purpose of verifying whether the claimed LF anomalies (Stetson 1991, Faulkner & Swenson 1993, Bolte 1994 and Langer et al. 2000) were real or not. We also attempted a determination of the cluster ages from the shape of the SGB peak, and from this we inferred a value for the cluster distance. Our main conclusions are the following:

- No SGB hump is found in any of our GGCs. We showed that a very similar feature is present in the most crowded regions of our clusters, and therefore we conclude that it has to be interpreted as an artifact of stellar blending;
- The observed number of MS/RGB stars is on average in good agreement with theoretical predictions in all the explored metallicity range;
- There is no statistically significant excess of stars in the observed upper RGB LF, at any metallicity;
- A difference in the slope of the upper RGB LF of the most metal rich clusters ( $[M/H] > -0.7$ ) is likely to be due to errors in the bolometric corrections for extremely red stars. Indeed, also the CMD of such metal rich clusters do not agree with theoretical models in the upper RGB region, for the same reason;
- Although in principle the shape of the SGB allows the determination of the cluster age, in practice the method is strongly affected both by errors in the metallicity, and, even more, by the quality of the photometry. Keeping in mind this uncertainty, we find a mean age of 13 Gyr, without any trend with metallicity.
- The cluster distances we obtain after imposing the ages derived above are on average in good agreement with the distances quoted in the latest revision of the Harris catalog, the difference being  $(m - M)_V^{LFs} - (m - M)_V^{HARRIS} = -0.01 \pm 0.15$ .
- We find a systematic difference of  $\sim 0.26$  magnitudes between the empirical and theoretical absolute magnitude of the RGB bump, with the exception of the models by Gi-

<sup>1</sup> The distances in the latest issue of the Harris catalog are computed from the observed mean magnitude of the HB, adopting the relation  $M_V(HB) = 0.15[Fe/H] + 0.80$ .

rardi et al. (1999). The discrepancy disappears if we adopt the longer distance scale obtained from theoretical ZAHB models (Cassisi et al. 1999).

*Acknowledgements.* We want to thank the referee, Alvio Renzini, for his helpful comments and discussions, which surely improved in many aspects this paper. We are indebted with Alessandro Chieffi, for having provided the programs to interpolate within the grid of the Straniero et al.'s models, and to Paolo Ventura, who specifically calculated the models for the most metal-rich clusters. We also thank Leo Girardi and Peter Stetson for many useful discussions. It is a pleasure to thank Santino Cassisi for being constantly available for discussions and suggestions, and Giuseppe Bono for useful comments on the original manuscript. This work was supported by MURST under the project: "Stellar Dynamics and Stellar Evolution in Globular Clusters". Partial support by ASI is also acknowledged.

## References

- Armosky B.J., Sneden C., Langer G.E., Kraft, R.P., 1994, *AJ* 108, 1364  
 Bergbusch P., Vandenberg D.A., 1992, *ApJS* 81, 163  
 Bolte M. 1994, *ApJ* 431, 223  
 Bressan A.G., Chiosi C., Bertelli G., 1981, *A&A* 102, 25  
 Carretta E., Gratton R.G., 1997, *A&AS* 121, 95  
 Cassisi S., Salaris M., 1997, *MNRAS* 285, 593  
 Cohen J.G., Gratton R.G., Behr B.B., Carretta E., 1999, *ApJ* 523, 739  
 Degl'Innocenti S., Weiss A., Leone L., 1997, *A&A* 319, 487  
 Djorgovski S.G., 1993, In: Djorgovski S., Meylan G. ASP (eds.) *Structure and Dynamics of Globular Clusters*, Conf. Ser. 50, San Francisco: ASP, p. 373  
 Faulkner J., Swenson F.J., 1993, *ApJ* 411, 200  
 Fusi Pecci F., Ferraro F.R., Crocker D.A., Rood R.T., Buonanno R. 1990, *A&A* 238, 95  
 Girardi L., Bressan A., Bertelli G., Chiosi C., 1999, *A&A*, in press (astro-ph/9910164)  
 Harris W.E., 1996, *AJ* 112, 1487  
 Hesser J.E., McClure R.D., Hawarden T.G., et al., 1984, *PASP* 96, 406  
 King C.R., Da Costa G.S., Demarque P., 1985, *ApJ* 299, 674  
 Langer G.E., Bolte M., Sandquist E., 2000, *ApJ* 529, 936  
 Ortolani S., Barbuy B., Bica E. 1990, *A&A* 236, 362  
 Ortolani S., Bica E., Barbuy B., 1992, *A&AS* 92, 441  
 Piotto G., Sosin C., King I.R., 1997, In: Rood R.T., Renzini A. (eds.), *Advances in Stellar Evolution*, Cambridge: Cambridge University Press, p. 84.  
 Piotto G., Zoccali M., King I.R., 1999a, *AJ* 117, 264  
 Piotto G., Zoccali M., King I.R., 1999b, *AJ* 118, 1737  
 Piotto G., Zoccali M., 1999, *A&A* 345, 485  
 Ratcliff S.J., 1987, *ApJ* 318, 196  
 Renzini A., Fusi Pecci F., 1988, *ARA&A* 26, 199  
 Rich R.M., Sosin C., Djorgovski S. G., et al., 1997, *ApJL* 484, L25  
 Rood R.T., Crocker D.A., 1989, In: Schmidt E.G. (ed.), *The Use of Pulsating Stars in Fundamental Problems of Astronomy*, IAU Coll. 111, ed. Cambridge UK: Cambridge U. Press, p. 103  
 Rood R.T., Carretta E., Paltrinieri B., et al., 1999, *ApJ* 523, 752  
 Salaris M., Cassisi S., 1998, *MNRAS* 298, 166  
 Salaris M., Chieffi A., Straniero O., 1993, *ApJ* 414, 580  
 Salaris M., Weiss A., 1998, *A&A* 335, 943  
 Sandquist E.L., Bolte M., Stetson P.B., Hesser J.E. 1996, *ApJ* 470, 910  
 Silvestri F., Ventura P., D'Antona F., Mazzitelli I., 1998, *ApJ* 509, 192  
 Sosin C., Piotto G., King I.R., et al., 1997a, In: Rood R.T., Renzini A. (eds.), *Advances in Stellar Evolution*, Cambridge: Cambridge Univ. Press, p. 92  
 Sosin C., Dorman B., Djorgovski S.G., et al., 1997b, *ApJ* 480, L35  
 Stetson P.B., 1991, In: Janes K. (ed.), *The Formation and Evolution of Star Clusters*, ASP Conf.Ser. 13, San Francisco: ASP, p. 88  
 Straniero O., Chieffi A., Limongi M., 1997, *ApJ* 490, 425  
 Sweigart A.V., 1997, *ApJ* 474, L23  
 Sweigart A.V., Gross P.G., 1978, *ApJS* 36, 405  
 Sweigart A.V., 1998, In: Philip A.G.D., Liebert J., Saffer R.A. (eds.) *The Third Conference on Faint Blue Stars*, Cambridge: Cambridge Univ. Press, p. 3  
 Rosenberg A.R., Saviane I., Piotto G., Aparicio A., 1999, *AJ* 118, 2306  
 Vandenberg D.A., Larson A.M., DePropris R., 1998, *PASP* 110, 98  
 Zoccali M., 1999, *Tesi di Dottorato di Ricerca*, Università di Padova  
 Zoccali M., Cassisi S., Piotto G., Bono G., Salaris M., 1999, *ApJ* 518, L49  
 Zoccali M., Cassisi S., Bono G., et al., 2000, *ApJ*, in press